IEEE Access
Multidisciplinary | Rapid Review | Open Access Journal

Received March 11, 2019, accepted March 29, 2019, date of publication April 4, 2019, date of current version April 18, 2019.

Digital Object Identifier 10.1109/ACCESS.2019.2909321

A Novel Modeling for Assessing Frequency Behavior During a Hydro-to-Thermal Plant Black Start Restoration Test

ROBERTO BENATO[1], (Senior Member, IEEE), GIANLUCA BRUNO[2], SEBASTIAN DAMBONE SESSA[1], (Member, IEEE), GIORGIO MARIA GIANNUZZI[2], LUCA ORTOLANO[2], GIANNI PEDRAZZOLI[1], (Member, IEEE), MICHELE POLI[2], FRANCESCO SANNITI[1], (Member, IEEE), AND ROBERTO ZAOTTINI[2]

[1]Department of Industrial Engineering, University of Padova, 35131 Padua, Italy
[2]Terna S.p.A., 00156 Rome, Italy

Corresponding author: Roberto Benato (roberto.benato@unipd.it)

ABSTRACT Northern electric grid of Italy was involved in a black start mock drill. This test took place on November 2016 in order to check the coordination and efficiency of all the operational staffs and the automatic regulators involved in the case of a real blackout scenario. This paper presents the results of a research carried out in collaboration with Terna Rete Italia (the Italian Transmission System Operator), in order to find strengths and weaknesses and eventually to upgrade the existing restoration plan. Starting from the measures coming from generating plants and substations bars, the model of frequency regulation system for both the participating hydro and thermal power plants is developed. This work gives the system operator an essential tool to understand many complex dynamics and phenomena occurred during the test. At the same time, a robust model simulating the system behavior with different grid configurations is presented: it gives the opportunity to enhance both the classical power system control theory and the black start practices.

INDEX TERMS Blackout, black start, grid restoration, frequency regulation.

I. INTRODUCTION

In the last years, the rapid growing of distributed generation has drastically modified the operation functioning of power systems. New needs have arisen in terms of observability, reachability and control besides highlighted critical issues due to the inverter-based generation with a subsequent decreasing of synchronous rotating inertia: the different dynamic behavior of loads have triggered different network regulations. For these reasons, the international activity is very intensive both at normative level (including the national program of distributed generation retrofit) and at operating level for adapting the defense, control and regulation systems to the novel grid reality. The abovementioned situation must be framed in the scenario of climate changes, which dramatically intensifies the violence, and the impact of these stresses on electrical systems [1]–[3].

The associate editor coordinating the review of this manuscript and approving it for publication was Zhiyi Li.

Analogously, besides the preventive and curative countermeasures, it is necessary to conceive strategies and restoration plans adapted to the new system paradigm: this ought to guarantee an electricity service recovery as quick and safe as possible in case of outage more or less wide.

The restoration tests constitute the chief tool in order to verify the real validity of restoration strategies. By means of these tests it is possible to verify that all foreseen procedures are correctly implemented and, at the same time, to verify the robustness of the developed mathematical modeling. The tests are performed by means of intentional and controlled black-out along the chief electric backbones; the involved power plants make all the necessary procedures in order to recover the normal operating conditions in the shortest possible time.

Together with the analysis and simulation tools which are normally used by TERNA both during the preparation of a test and during the study and verification ex post, a project has been undertaken in order to build a Matlab-Simulink

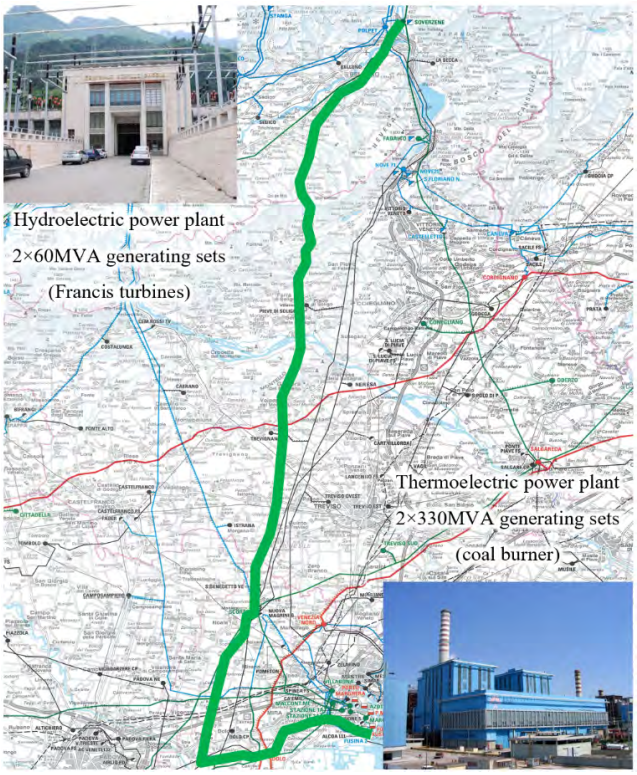

FIGURE 1. Black start mock drill geographical area and power plants involved.

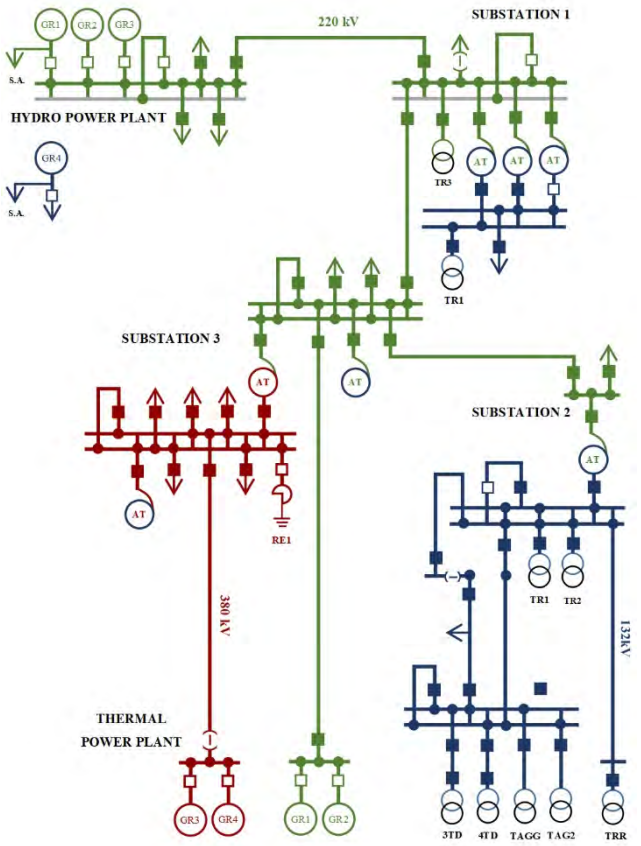

FIGURE 2. Simplified scheme of the island grid during the mock drill.

environment exclusively devoted to the simulation of the restoration test. This simulation environment, complementary to the grid simulator, gives the possibility to check, validate and quickly modify the system modeling used to plan the restoration tests. From the black start mock drill standpoint, papers [2], [4]–[11] report the procedures followed during the black start of different power plants and provide several measurements performed during these exercises. The aim of these works is to verify the efficiency of the followed procedures and to analyze the weak points that have emerged during the mock drills. Other interesting contributions focus on innovative strategies to plan the black start of electrical grids [12] or micro-grids, [13]–[15] even by exploiting energy storage installations [16], [17]. In this paper, authors exploit the frequency measurements carried out during a hydro-to-thermal power plant black start mock drill in order to develop a model in Matlab Simulink environment able to correctly represent the black start frequency behavior. The aim of this work is to verify if the classical theory of power systems control can [18]–[25] be effectively applied to correctly foresee the behavior of the systems involved in a black start process. By comparing the frequency simulation results with the experimental frequency measurements, it has been possible to observe how the classical transfer functions commonly used in power system control are not sufficient to correctly represent the real dynamics of power plant black starts. This fact could lead to significant mistakes if a black start plan was designed on the basis of the traditional modeling procedure.

In particular, the transfer function of the local integral control has been improved in comparison with that proposed in technical literature [22]–[25]. In the paper, a more complete Local Integral Controller (LIC) transfer function has been presented and integrated in a model representing the whole complex system involved in the black start process. The combination of all the key elements which constitute a single generating plant such as speed transducers, actual speed regulators, error signal amplifiers, servomotors and controlled valves for both steam and water turbine supply, has been taken into account in the model. The frequency regulator model has been developed consistently with the actual frequency regulator characteristics reported in [26]–[31].

II. BLACK START MOCK DRILL IN THE NORTHERN ITALY

The involved portions of 380, 220 and 132 kV transmission grids (see Fig. 1 and 2), which supply distributed loads through a sequential connection of several transformers, a hydro power plant along with a thermal power plant (see Fig. 1) which holds the lead role. In this specific case, the voltage regulation has been disregarded since there is an almost perfect unbundling between frequency and voltage due to the very low r/x involved transmission lines. The test was carried out in five stages, which are shown in Fig. 3 and 5 with reference to the behavior of the active power generated

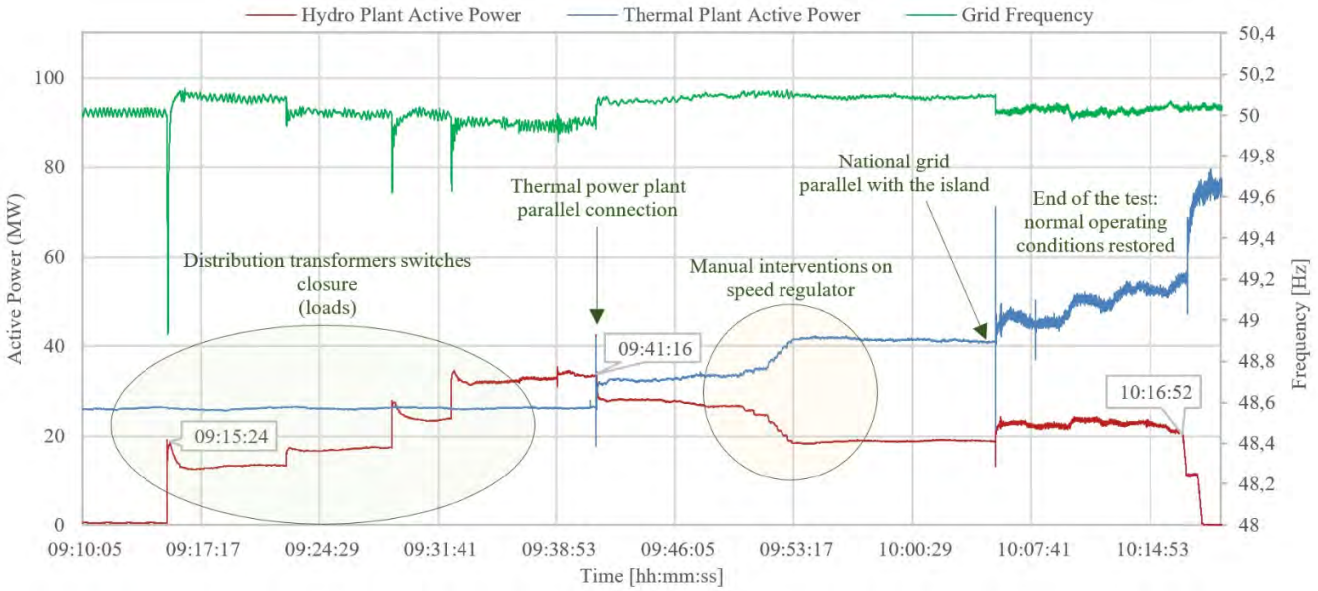

FIGURE 3. Grid frequency and active power flows during the test (different steps of the mock drill are shown in correspondence of these behaviors).

by the two power plants and the grid frequency. These stages are:

1) At 7:00 a.m. the thermal power station reduced its production going out from the automatic implementation system of production plans.

The station has been switched off from the national electric grid (black-out simulation) in a condition of load rejection but guaranteeing the supply of its auxiliary services.

1) At 8:00 a.m. the external auxiliary service supply has been made unavailable for all the primary stations involved. In these conditions, the scheduled network structure has been set to safely perform the restoration test.
2) At 8:45 a.m. all the generating sets have been stopped in the hydro power station; both the auxiliary systems and the central bars have been disconnected from the national transmission grid.
3) The fourth part consisted in the black start of two generating sets of the hydro power station by means of a 290 kW Francis turbine (see Fig. 4) reserved to auxiliary system emergency supply. Once the nominal speed has been reached, the closure of the first group circuit breaker has allowed the energization of the restoration backbone (starting voltage); after this, the closure of the second group circuit breaker has occurred by means of parallel control. In order to allow the thermal power plant to give the network active power (anti motoring action load) in the moment of parallel connection, about 40 MW of distributed loads were connected to the restoration backbone. This step closes with the parallel connection between thermal power plant and the island (including the hydro power plant).

FIGURE 4. Emergency generating set reserved for hydro power plant auxiliary systems.

4) During the final phase of the mock drill, the parallel between the island and the rest of the national transmission network has been carried out.

III. BRIEF THEORETICAL RECALLS OF PRIMARY AND SECONDARY FREQUENCY REGULATIONS

A. FREQUENCY CONTROL IN RESTORING PROCESS

The frequency deviations in a power systems should be as small as possible (maximum tolerable deviation of $\pm$ 100 mHz in the Italian network) to ensure the correct operation of its generating units and loads. Frequency and active power are strictly linked quantities in an electrical transmission system. Both rotating generation units and loads have a frequency-power dependence due to an obvious relation with the mechanical speed [29].

Frequency regulation can be considered as divided into three different kinds of control.

Primary frequency control (i.e. the frequency containment process) guarantees a constant containment of frequency

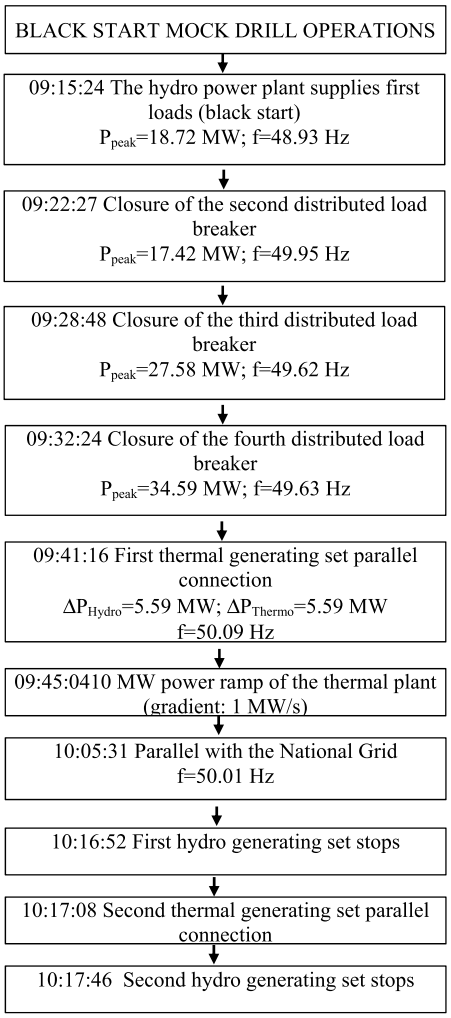

FIGURE 5. Overview scheme of the mock drill operations.

deviations (fluctuations) from the nominal value. By the joint action of all the interconnected parties, primary control stabilizes the system frequency at a stationary value after a disturbance or incident (loss of generation or increase/decrease of the load) in the period of seconds (typically 30 s), but without restoring the nominal frequency (static frequency deviation).

The purpose of the secondary frequency control (i.e. the frequency restoration process) is therefore to bring back the frequency to its nominal value, so restoring the generation margin served by the primary regulation and at the same time guaranteeing the agreed exchanges with the other grids. This control acts on the speed governor by modifying the active power of the generation sets typically in the period of some minutes [29]–[31].

During the restoration process following a blackout, in the island system that is created, the secondary regulation function managed by the TSO on a national level becomes unavailable since the system is not sound and the power plant involved in the restoration procedures is part of an autonomous islanded network. For this reason, black start addicted power plants (and in general all the power plants

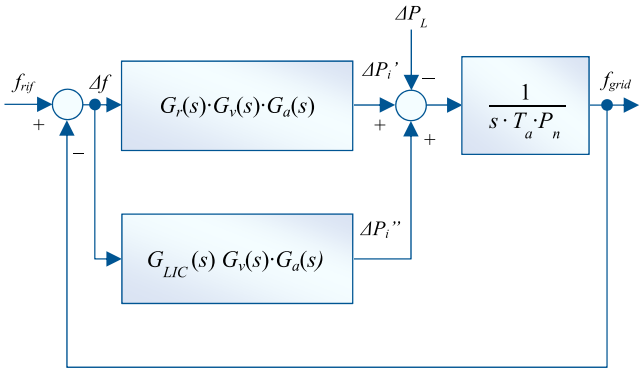

FIGURE 6. Linearized block diagram of the frequency regulation of a generating unit.

with a rated power greater than 10 MW according to the Addendum A15 of the Grid Code) must implement a Local Integral Controller (LIC). Its aim, similarly to the secondary frequency control, is to locally regulate the active power supplied by a generating set, until the deviation between real and nominal frequency gets under a pre-set value.

Eventually, the tertiary control (i.e. the replacement reserves) consists in recovery of the generation margin enslaved to the regulations [19], [20]. Therefore, secondary and tertiary control are not of interest for this study, since they do not affect the automatic regulation system of a power plant during a restoration process.

B. PRIMARY AND LOCAL INTEGRAL CONTROLLER BLOCK DIAGRAMS

Fig. 6 shows the block diagram in Laplace domain of a speed-frequency linearized feedback control, consisting of two coexisting feedback loops, one for primary frequency control and one for the LIC. Δf, ΔP_i and ΔP_L identify the Laplace transforms of the frequency variations (in Hz), of the variations of the mechanical power generated by the turbines (in MW) and of the variations of the active power absorbed by the loads (in MW) respectively.

In other words, ΔP_L represents the disturbance occurring in the network, which triggers the frequency control operation. ΔP_i in Fig. 6 is discomposed in the primary and the LIC power contributes ($\Delta P_i'$ and $\Delta P_i''$) supplied by the power plants to assess the primary frequency control and the LIC one. In fact, after a disturbance, the grid frequency must be brought back to the desired value or to a value close to it by the control system. The real core of the frequency control system lies on the $G_r(s)$ transfer function, which is related to the primary frequency control given by:

$$G_r(s) = \frac{\Delta\theta/\theta_n}{\Delta f} = \frac{1}{f_n \cdot b_p'} \frac{1+sT_2}{1+sT_1} = \frac{1+sT_2}{b_p' + sT_2 b_t'} \quad (1)$$

where:

- $T_1 \cong 15$ s (in case a standard hydro power plant [10]) is the first order pole time constant;
- $T_2 \cong 5$ s (in case of a standard hydro power plant [18]) is the first order zero time constant;

- b'$_p$ is the permanent generating set droop level, with a fixed value of 4%, according to the Grid Code [21];
- b'$_t$ is the transient droop level, sensed from a generating set in the instants immediately after a disturbance (in order to reduce the stress that the generating set has to endure);
- $\Delta\theta/\theta_n$ represents the degree of openness of the valve control system, where θ_n is the maximum openness of the valve;
- f_n is the nominal frequency of the system.

In the past, regulators and amplifiers were mechanical-hydraulic, electromechanical or electro-hydraulic: now, they are electrical or electronic. For this reason, few years ago, it would have been necessary to consider complex regulator schemes with accelerometer, transient feedback or temporary droop. Nowadays, $G_r(s)$ is reduced to a proportional derivative contribute for the primary regulation function or to a mere integrative action for automatic integral regulation function [22]–[25]. The LIC frequency control is represented in Fig. 6 by the local integral controller, whose transfer function $G_{LIC}(s)$, commonly used in literature, is given by:

$$G_{LIC}(s) = \frac{1}{f_n}\frac{K_I}{s} \tag{2}$$

where K_I is the integral controller gain, commonly set to 0.01 [19]–[21]. The functions $G_v(s)$ and $G_a(s)$ in Fig. 6 take into account the response time of the turbine valve control and of the turbine supply system respectively. Eventually, in order to consider the rotating inertia of the system, a third block needs to be added. It consists of an ideal integrator with two coefficients T_a and P_n characterizing the generating set start time and the nominal power respectively.

IV. MODEL DEVELOPMENT

In this section, the modeling procedures developed to represent the black start process described in Sect. 2 is expounded. The modeling process consists of two different steps. The first step implements a simple model with a single generating plant control. The second step enhances the first basic model towards a complete one, by taking into account:

- all parallel connections and disconnections of the generating sets;
- both primary and local integral frequency controls;
- the operator manual interventions on speed regulators [26]–[31].

The active power trend measured on the hydro power station bars is set up as a disturbance. The subsystem representing the generating set inertia (explained in the previous section) shows a start time coefficient T_a of 8.5 s for the thermal power plant. Differently, for the hydroelectric power plant the T_a coefficient is equal to 12.5 s. This value, taken from hydro generating set datasheet, is unusual: although plants of this kind have start time values between 8 and 10 s, this specific hydro power plant has the structural peculiarity of a heavily increased rotating inertia. The primary and LIC frequency control transfer functions are implemented by considering the parameters extracted from the regulator datasheet. In order to replicate the restoration process described in Sect. 2, the control system models of the two power plants are joined in a unique model, to observe how the two systems interact with each other. The models of the generating units are managed independently from each other, so that the contribution of each generating set can be highlighted on the basis of how many rotating elements are instantly connected. The complete final model overview is represented in Fig. 7. All the block functions inserted in the model are built separately, in order to keep every contribution visible. The TF1 subsystem includes all the manual interventions executed by the plant operators on thermal plant production level and the auxiliary system power absorptions. The latter needs to be considered since, for the duration of the test, the thermal plant was not turned off, but kept in a condition of load rejection. The two central subsystems TF2 and TF3 represent the real core of the model. The first describes the feedback control of the thermoelectric plant, whereas the second represents the hydroelectric one. The structure of the regulation system is not very different between the two power plants: they differ for the calibration values of the regulators and for the blocks representing the dynamics of the generating sets. Within each subsystem, there are two blocks simulating the primary regulation of each generating set and two blocks performing the integral regulation. In this case, the primary regulation was performed by both the two power plants, whereas only the hydroelectric plant provided for the integral regulation. All other smaller blocks within TF2 and TF3 are linked with the TF4 subsystem. It includes all the control logics, which pilot the two power plant blocks. All the logics hold in TF4 and the manual commands represented in TF1 are given as input data to the model. The correct timing of these operations can be accurately deduced from Fig. 3 and from scheme of fig. 5, which briefly summarize them. The TF5 subsystem represents the total rotating inertia of the system. As input, it receives the output values of the mechanical power from the subsystems TF2 and TF3, together with the values of the active power delivered by the power stations in the network. The latter data comes from the measurements at the power plant busbars. Rotating inertia, as well as the intervention of frequency regulation control functions, also depends on the effective presence of the generating sets. For this reason, TF5 is also linked to the control logic subsystem. The remaining blocks, external to the above mentioned subsystems, served as a monitoring to verify the correct construction of the model. They are used to calculate the average square deviation between the results of the simulation and the actual measurements on the network. The most interesting monitored quantities have been the grid frequency, the active power supplied by the hydroelectric plant and that supplied by the thermoelectric plant (as already shown in Fig. 3). Eventually, two blocks are used to transform the data provided in discrete time by the instruments into continuous time functions for the correct functioning of MATLAB/Simulink.

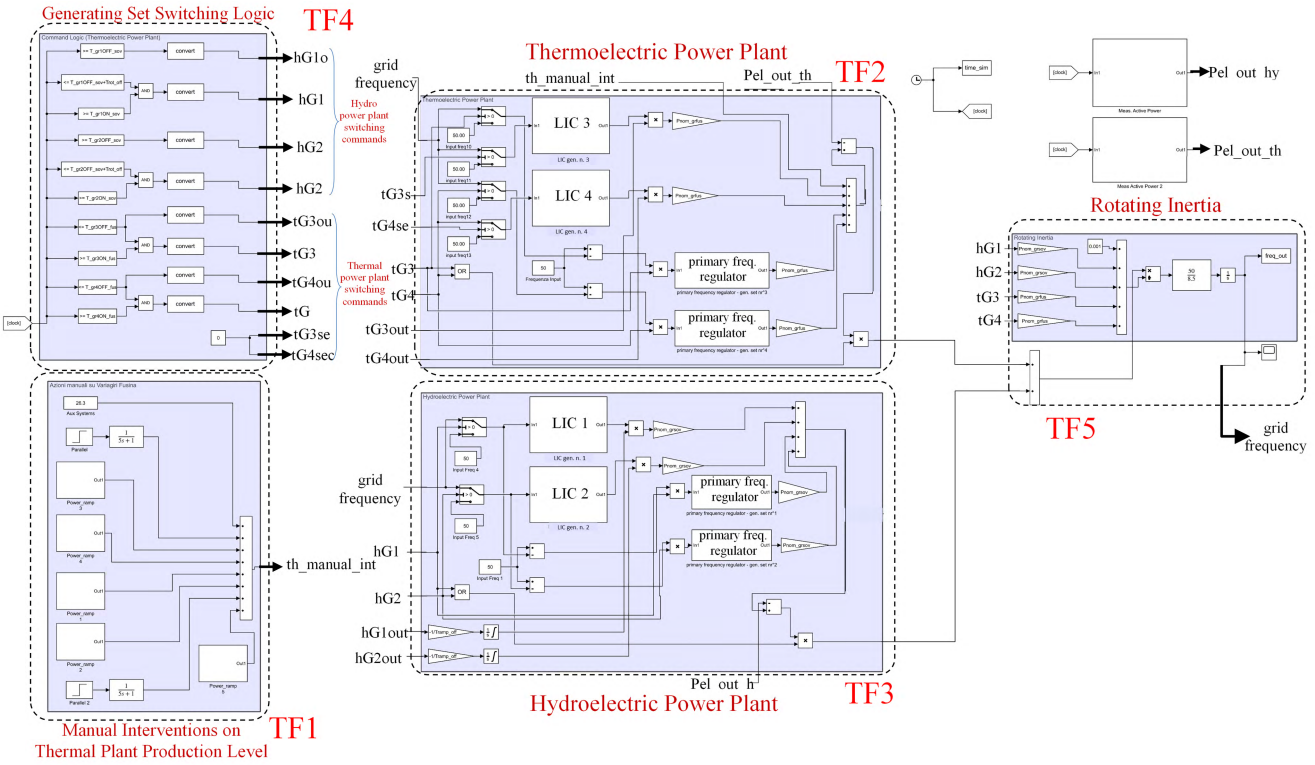

FIGURE 7. Final model overview on MATLAB/Simulink.

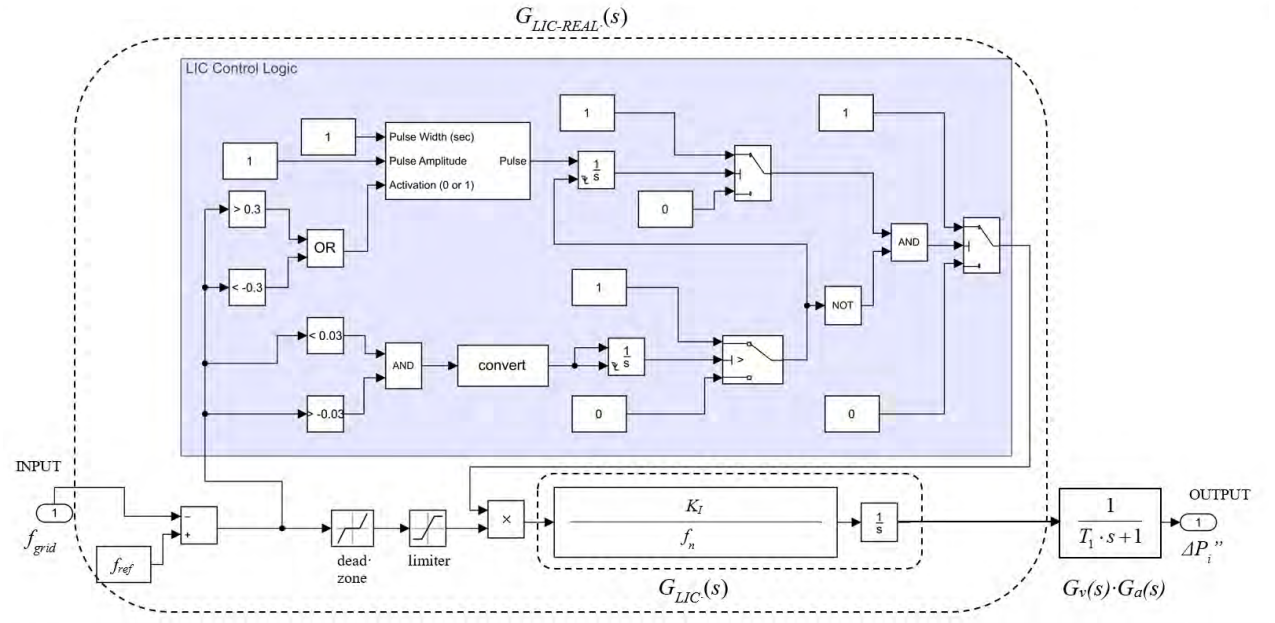

FIGURE 8. Detail of the final model: the Local Integral Controller block scheme.

A. THEORETICAL LIC BLOCK DIAGRAM VS. THE REAL ONE

An important achievement of this work consists in the creation of a block diagram for the LIC regulation system, which simulates the real operation (see Fig. 8).

A modeling process performed only on the basis of the classical control theory [18], [22]–[25], would have led this study to a negative result.

In fact, in the first instance, with the use of a LIC built with the classical formulation in (2), it was not possible to have

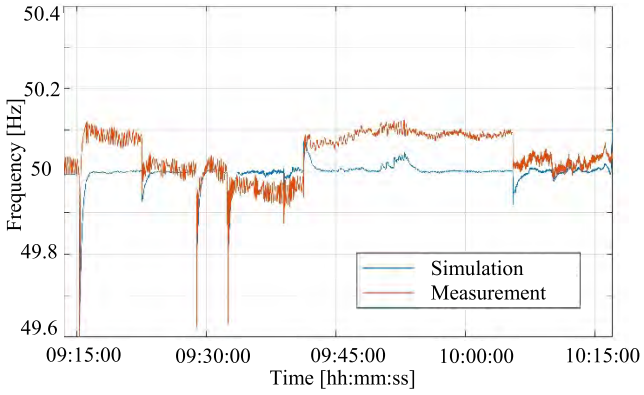

FIGURE 9. Grid frequency trend obtained by using the theoretical LIC transfer function taken from literature compared with measurements.

a good match between simulation and experimental data as shown in Fig. 9.

Only after a careful analysis of the involved generating groups and of the European standards for the frequency regulation systems [19], [20], it was possible to structure the complete model of a LIC whose behavior corresponded to the real one. In Fig. 8 the used LIC block scheme is represented.

The grid frequency f_{grid} subtracted from the frequency reference value f_{ref} determines the frequency error Δf. It is worth noting that the TSOs request that the LIC enters into operation only if Δf is out of a certain range of frequency [19], [20] namely R_f in the following, which is equal to ± 0.3 Hz for the Italian network.

Once the LIC is active, it integrates the frequency error until it falls inside a definite dead zone $D_f < R_f$, which is equal to ± 0.1 Hz in the Italian network.

Moreover, in real industrial applications the LIC must not overstress the supply control and the valve system. In order to satisfy this target, the limitation of the frequency error to a fixed value L_f is equivalent to set a maximum speed of variation of the power set-point required by the turbine.

This function is essential and always implemented in the real LIC systems. In light of this consideration, the $G_{LIC}(s)$ transfer function commonly used in literature is therefore only a part of the real one, namely $G_{LIC_REAL}(s)$ in the paper. In time domain, it can be expressed as a step-wise function, i.e.:

$$G_{LIC_REAL}(t) = \frac{k_I}{f_n} \int g_r(\Delta f) dt \tag{3}$$

where $g_r(\Delta f)$ can be expressed as:

$$g_r(\Delta f) = \begin{cases} L_f & if \ \Delta f > (L_f + D_f) \\ \Delta f - sgn(\Delta f) \cdot D_f & if \ |\Delta f| < L_f + D_f \\ & \wedge \ |\Delta f| \geq D_f \\ 0 & if \ |\Delta f| < D_f \\ -L_f & if \ \Delta f < -(L_f + D_f) \end{cases}$$

where K_I is set equal to 0.1.

$g_r(\Delta f)$ exists as soon as $-R_f > \Delta f > R_f$, i.e. when Δf falls outside of the R_f range. Matlab-Simulink environment allows user to pass easily from time domain equations to the Laplace domain ones.

V. RESULTS AND DISCUSSION

The comparison between the measured frequency behavior in the island grid and the simulated one is shown in Fig. 10 with a percent root mean squared error of 0.05 % i.e. 25 mHz. The figure impressively confirms the effectiveness of the described modeling.

In addition to the grid frequency behavior, the simulation also gives as output the active power generating level for each generating plant (see Fig. 11).

This second (and not less important) result shows how connected generating plants split between each other the total amount of active power required from loads. Like the previous frequency behavior, also the comparison between simulated active generating power and the measured one shows a negligible error (i.e. a root mean squared error of 0.59 MW). The highest deviation from the measured values occurred around 9:45 a.m., when the thermal plant operators manually acted on the regulator increasing the generating level. In the simulation, this event is represented by a power ramp, whereas in reality these hand-actions have been imparted in a completely arbitrary manner. However, this approximation is tolerable, because even if the power levels deviate from measurements during the manual interventions, after these, the measured active power and the simulated one return to match. The authors have performed many other comparisons concerning this restoration test (here not reported for the sake of brevity). They deal with an in-depth study of input and output values of each system sub-block. This also allows the authors to observe not only the dynamics of individual units, but also the separate contributions of the primary and secondary regulation control systems.

From the analysis of the model results compared with on-grid measures, the following considerations can be drawn.

A. INTEGRAL REGULATOR FAST RESPONSE

The development of a more complete and realistic LIC transfer function makes it possible to interpret easily the measurements.

As it is shown in fig. 12, by applying in (2) the commonly used gain $K_I = 0.01$, the LIC cut frequency is equal to 10^{-2} rad/s. This result does not justify the disturbances due to the resonance effects of penstock, caused by the pressure waves inside the penstock and surge tank, which are clearly visible in Fig. 10 in the form of rapid fluctuations in the measured frequency behavior [32]–[34]. In order to better understand this issue, Fig 13 shows the pressure graph sampled by probes installed at the penstock base: the ideally constant pressure value has two overlapped sinusoidal oscillations of about 15 s and 150 s (f $\cong$ 0.07-0.007 Hz). Therefore, on the basis of the LIC cut frequency computed by (2), the penstock resonance effect should be filtered by the LIC action.

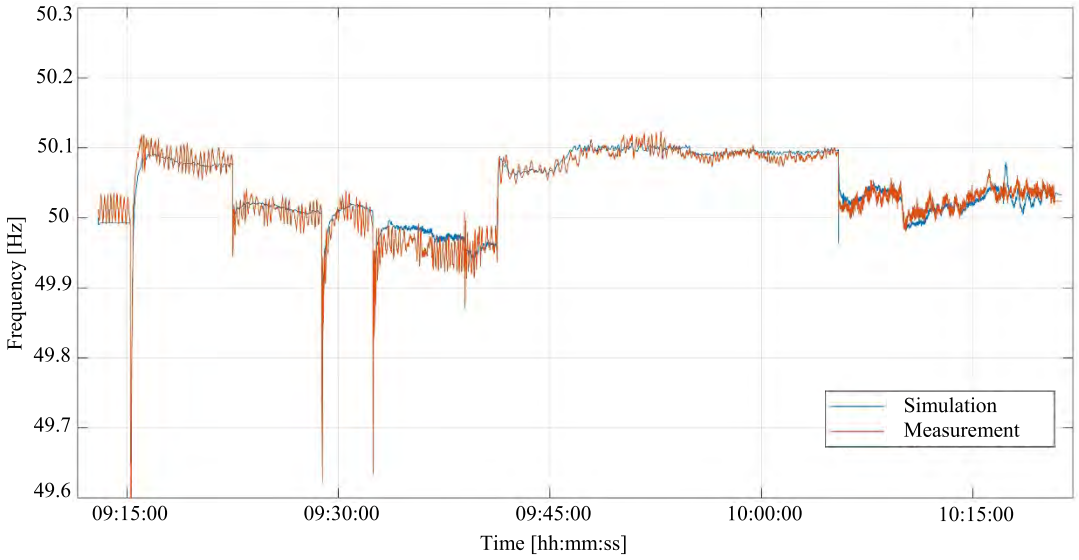

FIGURE 10. Grid frequency trend, comparison between simulation and real measurements.

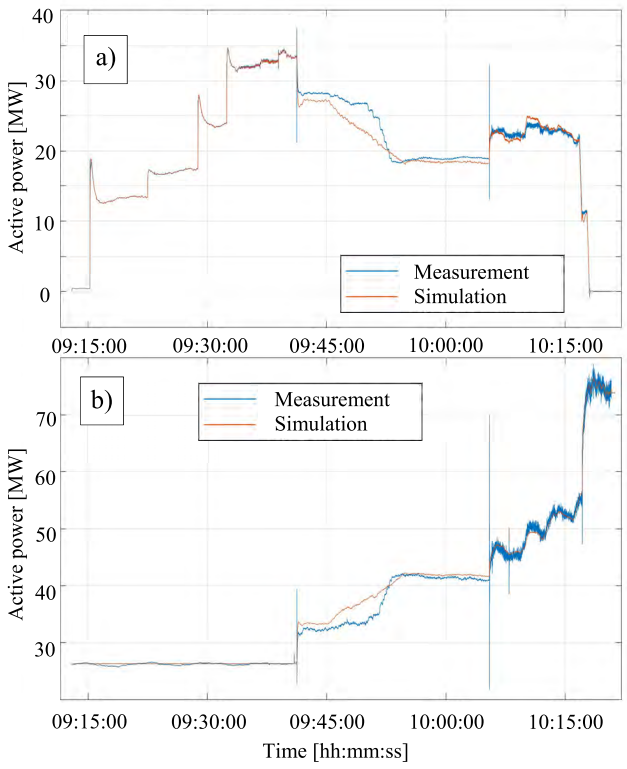

FIGURE 11. Comparison between simulation and measurements of the active power generated by a) hydro power plant and b) thermal power plan.

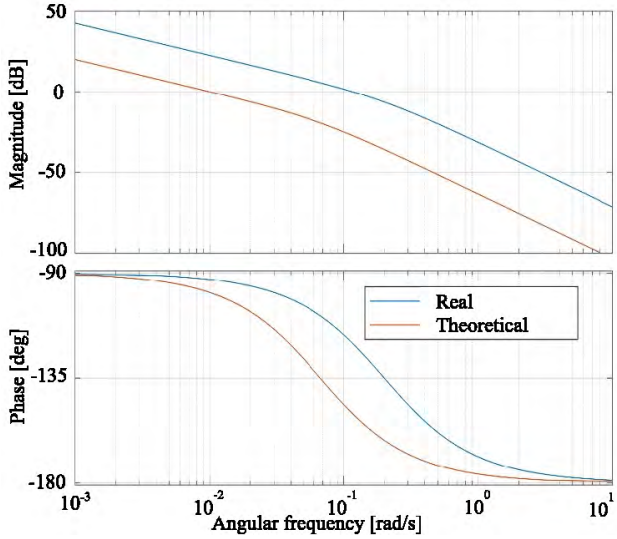

FIGURE 12. Bode diagram of the theoretical and the real frequency regulator.

The explanation of this effect has been found by implementing the actual LIC cut frequency value in the model by means of (3) and by changing the integration gain K_I from 0.01 to 0.1. This gain is affected by a series of refinements carried out at the power plant in order to guarantee the suitable readiness of the generating unit linked to a real power system. Therefore (as shown in Fig. 12) the LIC cut frequency in this case close to 10^{-1} rad/s (ten times higher than the theoretical one). Therefore, the response of the real integrator is clearly more reactive. Fig. 14 shows the difference in the simulation results by changing the K_I value. It is worth noting that if the traditional transfer function (2) was implemented by changing the gain K_I from 0.01 to 0.1, it would have not been sufficient to correctly represent the behavior of the system, and it would have not been possible to understand the reason behind the mismatch between measurements and model results, as it is shown in Fig. 15. Fig. 16 shows the importance of the LIC action by simulating a hypothetical situation without it: the frequency deviations would be such not to render possible the restoring the grid.

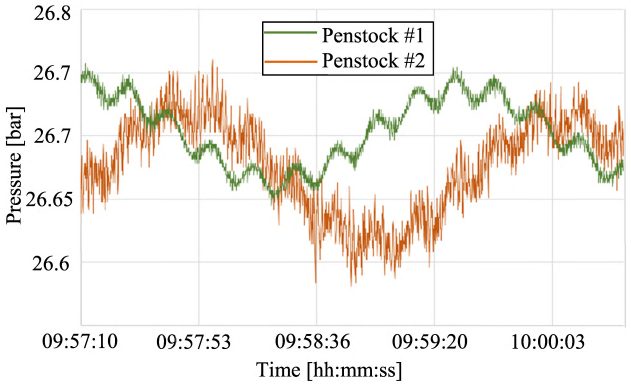

FIGURE 13. Pressure oscillations measured inside hydro power plant penstocks.

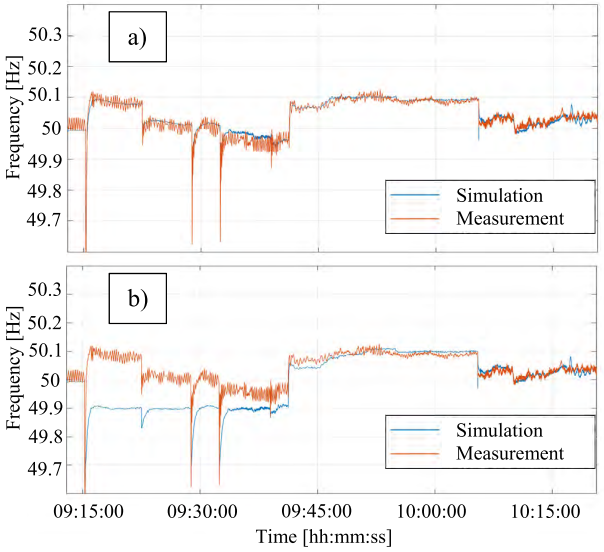

FIGURE 14. Comparison between simulated and measured frequency behavior by using a) the real K_I value and b) the theoretical one.

The presence of LIC is essential since it renders possible the synchronization of the island with the rest of national grid by means of the closure of the circuit breaker, which allows the connection between the two grids.

B. PENSTOCK RESONANCES

Although the developed model does not take into account the resonances generated by the pressure waves inside penstocks and surge tanks, there are no instability issues [32]–[34]. However, the presence of overshoot or undershoot phenomena is not negligible a priori. For this reason, a further development of the model is necessary by building a transfer function that simulates the influence of the penstock pressure waves on the frequency control system.

C. HIGHER DROOP THAN EXPECTED

The permanent droop of the thermal power plant is 10-11%, higher than the theoretical values reported in technical

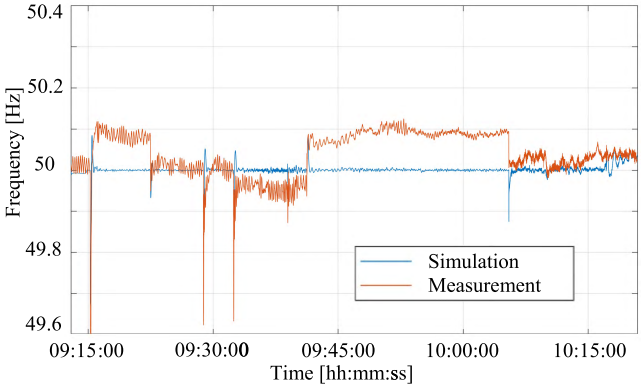

FIGURE 15. Grid frequency trend using the theoretical LIC transfer function formulation with $K_I = 0.1$.

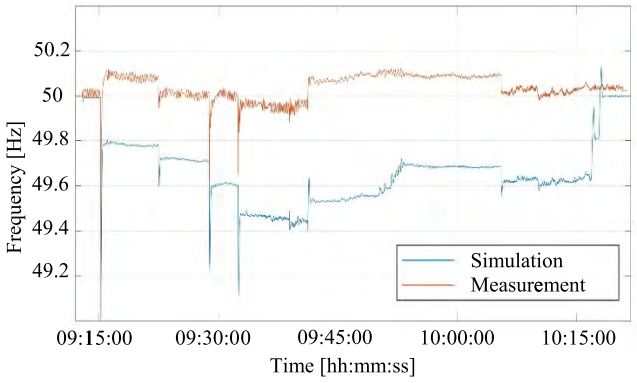

FIGURE 16. Frequency variations without the use of LIC.

literature [18] for typical operating points (generated power close to the rated one) but coherent with an operating point at minimum load.

D. GENERATING SET INSERTIONS

Power swings are the oscillations in active power flows consequent to the parallel insertion of a generating set on the island. In the first seconds from the parallel of the different sets, the simulated and measured active power do not match. In the simulations, in fact, the transient oscillations due to the set power swings are neglected.

From official test reports, it turns out that the thermal plant parallel connection was instantly followed by a production step up ranging between 8 and 12 MW in order to avoid returns of power from the grid. It is impossible to identify an exact value because this depends on many variables, such as the phase displacement between generator and grid at the time of connection, boiler pressure and temperature. The connection of a generating set and the power increase have been then represented by a simple first order step, because it is impossible to replicate a priori the power swings transient [37]–[41].

E. DISTRIBUTED LOADS BEHAVIOR

A fundamental consideration emerges from the observation of distribution transformers during the transient following

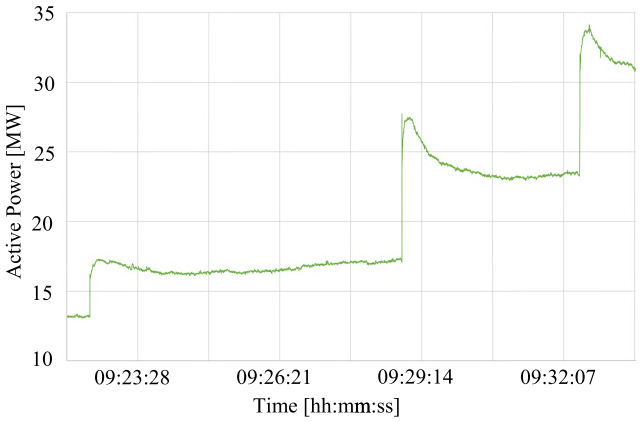

FIGURE 17. Detail of the active power highlighting distributed load behavior in the first instants of supply.

their connection to the island. Immediately after their connection, the absorbed active power rises up to 120% of their steady-state value (see Fig. 17) but, in some cases, up to 170 %. This phenomenon is common and well-known by TSOs: it occurs at the re-supply of the loads since, in the first instants, the coincidence factor increases. This absorption must be taken into account since it determines the under frequency transient. In the next instants, the power absorbed by the loads decreases due to the distributed generation, which automatically links to the grid. This phenomenon must be taken in due consideration when planning a restoration test: after the abovementioned peak, a nonlinear decreasing of the absorbed power can be observed in the transient. This behavior is due to the presence of distributed generation, which can power the network as soon as the voltage and frequency conditions allow it, without the need for a consensus from the system operator. The difficulty level during the planning phase of a restoration test further increases when consideration is given to the fact the some renewable resources (e.g. photovoltaic systems) follow weather conditions which may strongly vary during the hours of a day. For these reasons, it is fundamental for the TSO to know the exact size of the distributed generation that automatically comes into production as soon as the grid conditions allow it.

This is an essential requirement to adjust the total power supply level on black-start generating sets, so that main thermal plants can be re-started and restoration procedures can be correctly implemented [29]–[33]. In the technical literature, this topic is included in the ''observability'' and implies a knowledge of the distributed generation both at operating planning and at real time levels.

VI. CONCLUSIONS

This paper presents the process of implementation and validation of a MATLAB/SIMULINK (widely used by the authors also for other network models [43]–[49]) simulation tool of electromechanical transients associated to the restoration test: this tool joins the extremely powerful ones, which TERNA has developed in the last years in RME and EMT environments.

The added value of this tool potentially lies in the possibility of realizing and quickly validating the dynamic models which successively could merge into the grid simulator.

The agreement between SIMULINK model and measurements is extremely promising even if the penstock resonances of the hydroelectric power plant are not considered.

The chief conclusions derived from the Simulink model are:

- The approach used in the modeling of restoration backbone appears to be suitable;
- The presence of overshoot or undershoot phenomena due to pressure waves along the penstock is not negligible a priori even if, in this specific case, this phenomenon has not been cause of instability or bad results.

It is worth noting that the ratio r/x of the transmission lines involved in the mock drill are extremely low so that the frequency behavior depends prevalently upon the active power. However, further developments of the model require the implementation of the automatic voltage regulations, which, in turn, prevailingly depend on the reactive power. Moreover, this future enrichment and enhancement of the model will be validated by other restoration tests foreseen in Italy. The new European Rule 2017/2196 (Network Code Emergency and Restoration) places particular emphasis on studies, compliance checks and restoration tests: this practice has been consolidated in Terna for a long time and improved during the years in terms of accurateness of the models for studying and simulating and in terms of validation during the real restoration tests.

In the light of the results obtained from this research, in the future, the SIMULINK program could be used as propaedeutic and complementary but never replacing the real tests which allow gaining numerous data on the system functioning and on the capability of restoring the electric grid in short times.

REFERENCES

[1] K. Yamashita, J. Li, P. Zhang, and C.-C. Liu, ''Analysis and control of major blackout events,'' in *Proc. Power Syst. Conf. Expo.*, Seattle, WA, USA, Mar. 2009, pp. 1–4.
[2] *Cigré WG C2.21: Lessons Learnt from Recent Emergencies and Blackout Incidents*, document Technical Brochure # 608, 2015
[3] *Final Report of the Investigation Committee on the 28 September 2003 Blackout in Italy*, Union Coordination Transmiss. Electr., Brussels, Belgium, 2004.
[4] P. Mukhopadhyay *et al.*, ''Black start experiences for 400 kV hydro power plant in western regional grid of India,'' in *Proc. Nat. Power Syst. Conf. (NPSC)*, Bhubaneswar, India, Dec. 2016, pp. 1–6.
[5] M. Nagpal, T. G. Martinich, Z. Jiao, S.-H. Manuel, and H. A. Zhang, ''Lessons learned from a regional system blackout and restoration in BC hydro,'' *IEEE Trans. Power Del.*, vol. 33, no. 4, pp. 1954–1961, Aug. 2018. doi: 10.1109/TPWRD.2017.2768046.
[6] V. K. Agrawal, R. K. Porwal, R. Kumar, and V. Pandey, ''Mock blackstart drills—An excellent learning experience for power system operators,'' in *Proc. 5th Int. Conf. Power Syst. Protection Automat.*, Dec. 2010, pp. 6–9.
[7] Terna S.p.A., ''Piano di emergenza per la sicurezza del sistema elettrico (nuovo PESSE),'' Codice di Rete, Rome, Italy, Tech. Rep., 2005.
[8] V. K. Shrivastava, V. Pandey, A. P. Das, P. K. Sanodiya, S. Mohapatra, and R. Kumar, ''Black start experience for gas based power plant in Indian grid,'' in *Proc. IEEE Inter. Conf. Signal Process., Inform., Commun. Energy Syst.*, Kozhikode, India, Feb. 2015, pp. 1–5.

[9] Terna S.p.A., "Piano di riaccensione del sistema elettrico nazionale," Codice di Rete, Rome, Italy, Tech. Rep., 2006.

[10] Terna S.p.A., "Salvaguardia della sicurezza," Codice di Rete, Rome, Italy, Tech. Rep., 2017.

[11] Terna S.p.A., "Prescrizioni tecniche integrative per la connessione al Banco Manovra Interrompibili," Codice di Rete, Rome, Italy, Tech. Rep. A40, 2012.

[12] E. Lu, N. Wang, Z. Qin, H. Liu, and Y. Hou, "Black-start strategy for power grids including fast cut thermal power units," in *Proc. IEEE Power Energy Soc. Gen. Meeting (PES)*, Vancouver, BC, Canada, Jul. 2013, pp. 1–5.

[13] M. Nuschke, "Development of a microgrid controller for black start procedure and islanding operation," in *Proc. IEEE 15th Int. Conf. Ind. Inform. (INDIN)*, Emden, Germany, Jul. 2017, pp. 439–444.

[14] J. Liu, A. Chen, C. Du, and C. Zhang, "An improved method for black start of hybrid microgrids," in *Proc. 36th Chinese Control Conf.*, Dalian, China, Jul. 2017, pp. 9187–9192.

[15] Z. Xu, P. Yang, Z. Zeng, Y. Zhang, J. Peng, and Q. Zeng, "Study on black start strategy for multi-microgrids," in *Proc. IEEE Innov. Smart Grid Technol.-Asia (ISGT-Asia)*, Melbourne, VIC, Australia, Nov./Dec. 2016, pp. 144–148.

[16] A. M. El-Zonkoly, "Renewable energy sources for complete optimal power system black-start restoration," *IET Gener. Transm. Distrib.*, vol. 9, no. 6, pp. 531–539, 2015.

[17] W. Liu, L. Sun, Z. Lin, F. Wen, and Y. Xue, "Multi-objective restoration optimisation of power systems with battery energy storage systems," *IET Gener. Transm. Distrib.*, vol. 10, no. 7, pp. 1749–1757, 2016.

[18] R. Marconato, *Electric Power Systems*, vol. 2. Milan, Italy: CEI, 2002.

[19] E. N. O. T. S. O. F. E. (ENTSO-E), *ENTSO-E Operation Handbook, Appendix1: Load-Frequency Control and Performance*, Eur. Netw. Transmiss. Syst. Oper. Electr. (ENTSO-E), Brussels, Belgium, 2004.

[20] *ENTSO-E Operation Handbook, Policy 1: Load-Frequency Control and Performance*, Eur. Netw. Transmiss. Syst. Oper. Electr. (ENTSO-E), Brussels, Belgium, 2009.

[21] Terna S.p.A., "Partecipazione alla regolazione di frequenza e frequenza-potenza," Codice di Rete, Rome, Italy, Tech. Rep. A15, 2008.

[22] P. Kundur, *Power System Stability and Control*. New Delhi, India: McGraw-Hill, 2008.

[23] A. J. Wood and B. F. Wollenberg, *Power Generation, Operation and Control*, 3rd ed. Hoboken, NJ, USA: Wiley, 2014.

[24] J. Machowski, J. Bialek and J. Bumby, *Power System Dynamics: Stability and Control*, 2nd ed. Hoboken, NJ, USA: Wiley, 2008.

[25] I. J. Nagrath and D. P. Kothari, "Automatic generation and voltage control," in *Modern Power System Analysis*, 4th ed. New Delhi, India: McGraw Hill, 2011, pp. 320–351.

[26] F. P. Demello *et al.*, "Hydraulic turbine and control models for system dynamic studies," *IEEE Trans. Power Syst.*, vol. 7, no. 1, pp. 167–179, Feb. 1992.

[27] F. P. deMello, R. Mills, and W. B'Rells, "Automatic generation control part I—Process modeling," *IEEE Trans. Power App. Syst.*, vol. PAS-92, no. 2, pp. 710–715, Mar. 1973.

[28] F. P. deMello, R. Mills, and W. B'Rells, "Automatic generation control part II—Digital control techniques," *IEEE Trans. Power App. Syst.*, vol. PAS-92, no. 2, pp. 716–724, Mar. 1973.

[29] A. Bonfiglio, Francisco M. Gonzalez-Longatt, A. Labella, and R. Procopio, "Implementation of primary frequency regulation on fully rated wind turbine generators," in *Proc. Int. Conf. Energy Environ. (CIEM)*, Bucharest, Romania, Oct. 2017, pp. 316–320.

[30] A. Bonfiglio, F. Delfino, M. Invernizzi, A. Perfumo, and R. Procopio, "A feedback linearization scheme for the control of synchronous generators," *Electr. Powers Compon. Syst.*, vol. 40, no. 16, pp. 1842–1869, 2012.

[31] O. I. Elgerd, "The energy system in steady state—The control problem," in *Electric Energy Systems Theory: An Introduction*, 2nd ed. New York, NY, USA: McGraw-Hill, 1983, pp. 310–358.

[32] L. Chen *et al.*, "Optimization of governor parameters to prevent frequency oscillations in power systems," *IEEE Trans. Power Syst.*, vol. 33, no. 4, pp. 4466–4474, Jul. 2018. doi: 10.1109/TPWRS.2017.2778506.

[33] H. V. Pico, J. D. McCalley, A. Angel, R. Leon, and N. J. Castrillon, "Analysis of very low frequency oscillations in hydro-dominant power systems using multi-unit modeling," *IEEE Trans. Power Syst.*, vol. 27, no. 4, pp. 1906–1915, Nov. 2012.

[34] D. Rimorov, I. Kamwa, and G. Joós, "Quasi-steady-state approach for analysis of frequency oscillations and damping controller design," *IEEE Trans. Power Syst.*, vol. 31, no. 4, pp. 3212–3220, Jul. 2016.

[35] Terna S.p.A., "Criteri di taratura dei relè di frequenza del sistema elettrico," Codice di Rete, Rome, Italy, 2004.

[36] Terna S.p.A., "Piano di difesa del Sistema elettrico," Codice di Rete, Rome, Italy, 2004.

[37] P. Sonkar, A. K. Chandel, and O. P. Rahi, "Integrated tuning of PID-derivative load frequency controller for two area interconnected system," *Int. J. Eng., Sci. Technol.*, vol. 7, no. 3, pp. 42–51, 2015.

[38] D. Gautam, L. Goel, R. Ayyanar, V. Vittal, and T. Harbour, "Control strategy to mitigate the impact of reduced inertia due to doubly fed induction generators on large power systems," *IEEE Trans. Power Syst.*, vol. 26, no. 1, pp. 214–224, Feb. 2011.

[39] P. Sonkar, O. P. Rahi, K. S. R. Murthy, and S. R. Bhardwaj, "Integrated tuning of modified PID load frequency controller for two area interconnected system including renewable energy sources," *Proc. 7th IEEE Power India Int. Conf.*, Bikaner, India , Nov. 2016, pp. 1–6.

[40] C. Zhao, U. Topcu, N. Li, and S. Low, "Design and stability of load-side primary frequency control in power systems," *IEEE Trans. Autom. Control*, vol. 59, no. 5, pp. 1177–1189, May 2014.

[41] Z. Hainan *et al.*, "Automatic establishment and optimal selection of power system black start plans," in *Proc. China Int. Conf. Electr. Distrib.*, Xi'an, China, Aug. 2016, pp. 1–6.

[42] R. Benato, M. Forzan, M. Marelli, A. Orini, and E. Zaccone, "Harmonic behaviour of HVDC cables," *Electric Power Syst. Res.*, vol. 89, pp. 215–222, Aug. 2012. doi: 10.1016/j.epsr.2012.03.012.

[43] R. Benato and A. Paolucci, "Multiconductor cell analysis of skin effect in Milliken type cables," *Electr. Power Syst. Res.*, vol. 90, pp. 99–106, Sep. 2012. doi: 10.1016/j.epsr.2012.04.006.

[44] R. Benato and D. Napolitano, "Overall cost comparison between cable and overhead lines including the costs for repair after random failures," *IEEE Trans. Power Del.*, vol. 27, no. 3, pp. 1213–1222, Jul. 2012. doi: 10.1109/TPWRD.2012.2191803.

[45] R. Benato, S. D. Sessa, F. Guglielmi, E. Partal, and N. Tleis, "Zero sequence behaviour of a double-circuit overhead line," *Electr. Power Syst. Res.*, vol. 116, pp. 419–426, Nov. 2014.

[46] R. Benato, S. D. Sessa, L. Guizzo, and M. Rebolini, "Synergy of the future: High voltage insulated power cables and railway-highway structures," *IET Gener., Transmiss. Distrib.*, vol. 11, no. 10, pp. 2712–2720, 2016.

[47] R. Benato, S. D. Sessa, M. Forzan, M. Marelli, and D. Pietribiasi, "Core laying pitch-long 3D finite element model of an AC three-core armoured submarine cable with a length of 3 metres," *Electr. Power Syst. Res.*, vol. 150, pp. 137–143, Sep. 2017.

[48] R. Benato and S. D. Sessa, "A new multiconductor cell three-dimension matrix-based analysis applied to a three-core armoured cable," *IEEE Trans. Power Del.*, vol. 33, no. 4, pp. 1636–1646, Aug. 2018.

[49] R. Benato, S. D. Sessa, and M. Forzan, "Experimental validation of three-dimension multiconductor cell analysis by a 30 km submarine three-core armoured cable," *IEEE Trans. Power Del.*, vol. 33, no. 6, pp. 2910–2919, Dec. 2018.

ROBERTO BENATO (M'02–SM'17) was born in Venezia, Italy, in 1970. He received the Dr. Ing. degree in electrical engineering from the University of Padova, in 1995, and the Ph.D. degree in power systems analysis, in 1999. In 2011, he was appointed as an Associate Professor with the Department of Industrial Engineering, University of Padova. He has authored 160 papers and four books, edited by Springer, Wolters Kluwer, and China Machine Press. He has been a member of six Cigré Working Groups (WGs) and secretary of two Joint WGs and also a member of the IEEE PES Substations Committee. In 2014, he was nominated as a member of the IEC TC 120—Electrical Energy Storage (EES) Systems in the WG 4—Environmental Issues of EES systems. In 2015, he was nominated as a member of the IEC TC 115—High Voltage Direct Current (HVDC) Transmission for DC Voltages Above 100 kV, and as a member of the IEC TC 122—UHV AC Transmission Systems. He is a member of AEIT. In 2017, he was elected to the grade of Cigré Distinguished Member.

GIANLUCA BRUNO was born in Rome, in 1974. He graduated in electrical engineering from the University of Rome La Sapienza, in 1999. He joined the Italian Independent System Operator (GRTN), in 2001, where he was involved in the operational framework of electrical power systems. In 2005, he was with Terna S.p.A., the Italian TSO, where he was the Manager for design and realization of transmission lines and substations in the mid-center area of Italy. In 2012, he moved to the System Operation Department, where he was, in the beginning, the Manager for system protection, control, and monitoring and is currently the Manager for operational analysis: the main tasks of his responsibility are the design and realization of dispatching energy management systems, system defense plans, HVDC systems, grid code drafting, network studies, and the analysis of network events. He has a very good experience and knowledge of the TSO business at European level, achieved with an active participation in several Entso-e working groups and committees. He is also a member of the Technical Committee 11/7, Italian Electrotechnical Committee (CEI).

SEBASTIAN DAMBONE SESSA (M'14) was born in Venezia, Italy, in 1981. He received the Dr. Ing. degree in electrical engineering from the University of Padova, in 2010, and the Ph.D. degree in power systems analysis, in 2017. In 2017, he was appointed as a Postdoctoral Researcher at the Department of Industrial Engineering, University of Padova. His main fields of research are transmission line modeling, stationary electrochemical storage, and high-voltage direct-current installations. He has been a member of two Cigré WGs (B1.47 and B1.45) and is currently a member of Cigré WG B1.56—Cable Rating Verification. He is a member of AEIT.

GIORGIO MARIA GIANNUZZI received the Electrical Engineering degree from the University of Rome. Until 2000, he was with ABB, where he was in charge of network studies, protection, and control applications, with special reference to RTU apparatus and data engineering issues. Since 2001, he has been with Terna S.p.A. as an Expert in defense plans/systems, dynamic studies, protection, telecontrol, and substation automation. From 2004 to 2011, he coordinated the study, design, and activation of wide-area defense systems (including interruptible customers systems) and wide-area monitoring systems. Under his guidance, the main security energy management systems were designed and coded: they are actually in use at the National Control Centre (optimal power flow security, market-constrained optimal reactive power flow, dynamic security assessment tool, dynamic and static security verification software, and operator training simulator). He supervised the revision of main Italian Grid Code technical enclosures (primary and secondary frequency regulation, load shedding, protection and automation, and defense plans). Until 2009, he was a member of a UCTE Expert Group on Power System Stability. In 2010, he joined the ENTSO-E System Protection and Dynamics Group. Since 2014, he has been the Convenor, coordinating the European evaluation over Dispersed Generation impact on system security and load shedding guidelines. He is currently responsible for the Engineering Department, National Dispatching Centre.

LUCA ORTOLANO is currently responsible for the monitoring and testing the activities of the network code connection criteria (frequency range, voltage range, and so on) and ancillary services (FCR, FRR, voltage regulation, and so on) of power plants connected to the HV grid. He is also involved in active maintenance and development of the Italian network code related to technical connection requirements and testing procedures and in Technical ancillary services requirements and testing procedures. He has coauthored the battery storage technical specification: connection requirements, ancillary service requirements, and testing of the Terna's Battery Storage Project. He has also coauthored the synchronous generators technical specification: connection requirements, operational requirements, and testing of the three new Terna's synchronous generators. He gave technical support in the process of connection and request of derogation of new power plant or upgrading the existing ones. Eventually, he is technically responsible for the monitoring and testing of the unit connected to the Terna's SPS of the defense plan.

GIANNI PEDRAZZOLI (M'18) was born in Padua, Italy, in 1992. He received the Dr. Ing. degree in electrical engineering from the University of Padova, in 2017. He holds a research grant at the Department of Industrial Engineering, University of Padova. His main fields of research are frequency control systems in generating plants and protections systems of synchronous generators. He is a young member of CIGRÉ and AEIT.

MICHELE POLI was born in Trento, Italy, in 1974. He received the Dr. Ing. degree in electrical engineering from the University of Padova, in 2001. Since 2001, he has been with Terna S.p.A., where he deals with the analysis of the electrical phenomena in the HV networks, the prevention of anomalous operations of power transmission lines, and the issues related to the distributed generation. He is involved in the power plants restart planning and management and on the planning of the electrical network development.

FRANCESCO SANNITI (M'19) was born in Feltre, Italy, in 1994. He received the bachelor's degree in energy engineering from the University of Padova, where he is currently pursuing the Dr. Ing. degree in electrical engineering. His main field of research is dynamic modeling of frequency–voltage control systems for power system restoring. He is a young member of CIGRÉ and AEIT.

ROBERTO ZAOTTINI received the degree in electrical engineering from the University of Rome La Sapienza, in 1999. In 1997, he was with the EDP-Consultant in collaboration with Autostrade. In 2000, he was with the telecommunications company, Infotel, in association with Ericsson. Since 2001, he has been with the Italian TSO, Terna S.p.A., as an Expert in static and dynamic studies, defense plans/systems, and restoration strategies. He contributed to the implementation of new restoration strategies between different TSOs (total path over 1400 km up to large power plants and use of shunt reactors) through the coordination of all relevant actors and electromagnetic and electromechanical simulations. Until 2005, he was a member of the UCTE Expert Group on Power System Stability. Since 2010, he has been a member of the ENTSO-E System Protection and Dynamics (SPD) Group. In 2013, the SPD Expert Group has produced an ENTSO-E report—Dispersed Generation Impact on CE Region Security. He is a member of the Project Team of Advanced Use of HVDC Links in System Operations. He was the Italian Member of the Cigré Working Group—System Restoration Procedures and Practices. He is a member of the Cigré Working Group—Operating Strategies and Preparedness for System Operational Resilience.